Ca^{2+} Conduction by an Amino Acid-Gated Ion Channel Related to Glutamate Receptors[1][W]

Eric D. Vincill, Anthony M. Bieck[2], and Edgar P. Spalding*

Department of Botany, University of Wisconsin, Madison, Wisconsin 53706

Ever since homologs of mammalian ionotropic Glu receptors (iGluRs) were discovered in plants (Lam et al., 1998; Lacombe et al., 2001), their molecular-level functions have been an intriguing question. Particularly in need of a direct experimental test is the hypothesis that plant Glu receptor-like (*GLR*) genes encode ligand-gated channels like the $Na^+/K^+/Ca^{2+}$-permeable iGluRs, which mediate electrochemical signaling in animal central nervous systems (Traynelis et al., 2010). The hypothesis was suggested to account for the prevalence of nonselective cation currents across plant cell membranes (Demidchik et al., 2002, 2004) and the ionic events including a Ca^{2+} rise triggered by amino acids in plant cells (Dennison and Spalding, 2000). The Ca^{2+} permeability aspect of that hypothesis is especially important, because the influx mechanisms that generate cytoplasmic Ca^{2+} signals are not well defined at the molecular level (McAinsh and Pittman, 2009; Dodd et al., 2010; Spalding and Harper, 2011). Direct assays of GLR transport activities are needed to test the hypothesis, especially because no GLR is similar to an iGluR in the pore region (Davenport, 2002), which typically determines the ion selectivity of Glu receptors (Traynelis et al., 2010).

Animal iGluRs can be expressed and studied with voltage-clamp techniques after expression in *Xenopus* oocytes (Hollmann et al., 1989), but when this was done with an Arabidopsis (*Arabidopsis thaliana*) GLR, no amino acid-gated activity was observed (Roy et al., 2008). Transplanting the pore region of a GLR into an iGluR followed by expression of the chimeric protein in *Xenopus* oocytes was successful. In some cases, a plant GLR pore could form a Na^+, K^+, and Ca^{2+} conductance when placed in the context of an iGluR protein, indicating that GLRs may function like iGluRs (Tapken and Hollmann, 2008). The case was strengthened by finding that the large, transient membrane depolarization and rise in cytoplasmic Ca^{2+} triggered by Glu in wild-type plants (Dennison and Spalding, 2000) depended on *GLR* genes. Specifically, *glr3.3* mutants were found to be defective in their response to each of the six different amino acids (Ala, Asn, Cys, Glu, Gly, and Ser) effective in the root apices of wild-type seedlings (Qi et al., 2006). These results genetically linked ionic events, including Ca^{2+} transport, to GLRs but fell short of demonstrating GLR3.3 to be a Ca^{2+}-permeable channel. This is also a fair assessment of results obtained with *glr1.2* mutant pollen tubes (Michard et al., 2011).

A previous electrophysiological study of *glr3.4* hypocotyls showed that their cells responded poorly to Asn or Ser and the response to Gly was marginally affected (Stephens et al., 2008). Responses to Ala, Cys, and Glu were normal. These results were interpreted to mean that GLR3.4 was sensitive to the Asn, Gly, and Ser subset of amino acid agonists (Stephens et al., 2008). Direct experimental tests of this hypothesis and the Ca^{2+} permeability of a GLR3.4 channel are presented here.

RESULTS

Subcellular Localization of GLR3.4 Expressed in Mammalian and Plant Cells

Human embryonic kidney (HEK) cells are a standard functional expression system for mammalian iGluR channels (Chazot et al., 1999), displaying little or no endogenous amino acid-gated channel activity (Zhang and Huganir, 1999). Much important information about the molecular functions of iGluRs has been learned by studying them in HEK cells (Keinänen et al., 1990; Monyer et al., 1992; Dravid et al., 2008). Therefore, we transfected HEK cells with a plasmid carrying a GLR3.4-GFP fusion cDNA. The resulting fusion protein was shown by fluorescence microscopy (Fig. 1A) to adopt a pattern very similar to previously published examples of proteins that reached the plasma membrane of HEK cells (Christopher et al., 2007; Tang et al., 2007; Mikosch et al., 2009). The expression pattern of free GFP is shown for comparison (Fig. 1B). Arabidopsis plants stably transformed with the same cDNA controlled by the 35S promoter to increase signal intensity showed a cellular signal consistent with plasma membrane localization (Fig. 1C). Plasma membrane localization was expected, because *glr* mutants are defective in ligand-gated ion transport at the plasma membrane (Qi et al., 2006; Stephens et al., 2008). Plasmolysis of leaf cells in the transgenic plants produced Hechtian strands of plasma membrane connecting the protoplast to sites of adherence at

[1] This work was supported by the Division of Chemical Sciences, Geosciences, and Biosciences, Office of Basic Energy Sciences of the U.S. Department of Energy (grant no. DE–FG02–10ER15527 to E.P.S.).

[2] Present address: Department of Biology, Doane College, 1014 Boswell Avenue, Crete, NE 68333.

* Corresponding author; e-mail spalding@wisc.edu.

[W] The online version of this article contains Web-only data.

www.plantphysiol.org/cgi/doi/10.1104/pp.112.197509

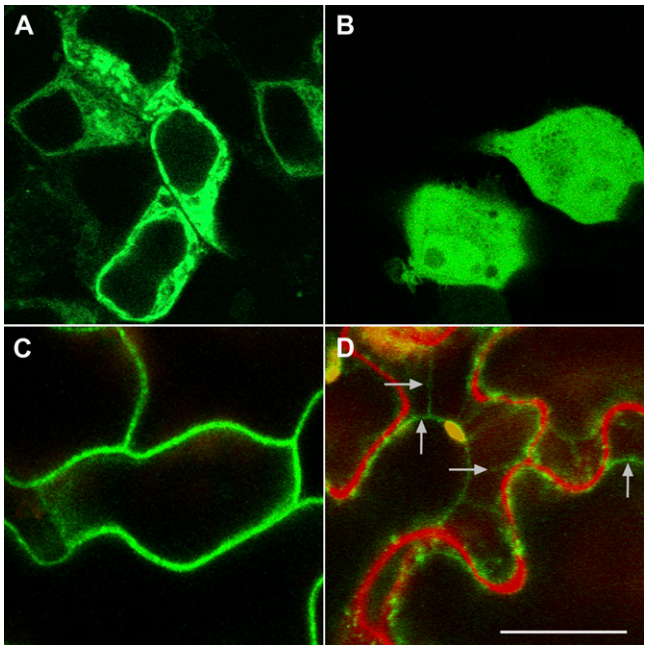

Figure 1. Plasma membrane localization of GLR3.4-GFP expressed in animal or plant cells. A, HEK cells transfected with a plasmid containing GFP fused to the carboxy terminus of the *GLR3.4* cDNA (pcDEST47-GLR3.4) showed signal throughout the cytoplasm and at the cell periphery, consistent with synthesis and maturation in the endomembrane system and delivery to the plasma membrane. B, Transfection of HEK cells with free GFP showed signal throughout the cell, including the nucleus. C, Arabidopsis plants stably transformed with *GLRL3.4-EGFP* driven by the 35S promoter showed signal at the periphery of leaf epidermal cells. D, Plasmolyzed *Pro-35S:GLR3.4-EGFP* leaf cells show GFP signal in the Hechtian strands of plasma membrane (horizontal arrows) that stretch between attachment sites in the cell wall (stained red with propidium iodide) and the plasma membrane surrounding the osmotically withdrawn protoplast (vertical arrows). Images are representative of at least six independent trials. Scale bar = 20 μm.

the cell wall. GFP signal was apparent in the Hechtian strands and in the plasma membrane surrounding the withdrawn protoplast (Fig. 1D). No evidence of chloroplast localization of GLR3.4 reported in a study that also reported plasma membrane localization (Teardo et al., 2011) was detected, though intense chlorophyll fluorescence could have masked a weak GFP signal.

The HEK cell result (Fig. 1A) indicated that a patch-clamp assay of ion transport across the plasma membrane was worth pursuing. The plant cell results (Fig. 1, C and D) indicated that any HEK cell results could be interpreted as relevant to the plant cell plasma membrane, where electrophysiological studies indicate the proteins function (Qi et al., 2006; Stephens et al., 2008).

Agonist Specificity

To test for ion channel function of GLR3.4, HEK cells were transfected with a bicistronic plasmid carrying GLR3.4 cDNA not fused to GFP and a separate open reading frame encoding a fluorescent marker protein. Fluorescent cells were subjected to patch clamp analyses. Whole-cell ionic currents across the plasma membrane were measured continuously with the membrane potential clamped at −70 mV. Switching to an Asn-containing bath solution induced a large inward current that sustained without significant desensitization over many seconds, returning to the pretreatment level upon washout (Fig. 2A). Cells transfected with a plasmid carrying only GFP did not respond to this treatment (Fig. 2A). The current trace in Figure 2B shows that Gly was approximately 50% as effective compared with Asn. Because the system displayed little desensitization, each test response could be normalized to that triggered by a strong Asn treatment administered to the same cell, thus accounting for any potential differences in GLR3.4 expression levels between cells. Figure 2C shows the magnitude of the response to each amino acid previously found to be an effective agonist in the wild-type plant (Qi et al., 2006; Stephens et al., 2008) plus the ineffective Phe relative to a preceding 1,000 μM Asn response. The GLR3.4 agonist specificity indicated by impaired electrophysiological responses of *glr3.4* mutants (Stephens et al., 2008) was confirmed by the behavior of GLR3.4 expressed in HEK cells. Asn and Ser were strong agonists, Gly less so, and the others not significantly different from Phe. Glu occupies the top position in the desensitization hierarchy in planta, probably by activating GLR3.3, but was a relatively poor agonist of GLR3.4 receptor channels, also as predicted by the earlier mutant studies (Stephens et al., 2008). Figure 2D shows that 10 μM of agonist produced a small response, which increased strongly over the concentration range previously found to be effective in plants (Dubos et al., 2003; Meyerhoff et al., 2005; Qi et al., 2006; Stephens et al., 2008). Across this concentration range, Asn and Ser were similarly strong agonists.

Ca^{2+} Permeability

The main ions in the solutions employed were Na^+ (140 mM inside/140 mM outside), Cl^- (140 mM inside/140 mM outside), and Ca^{2+}, which was either 2 mM or 20 mM outside and buffered at sub-micromolar levels inside by EGTA. To identify which of these ions was transported by GLR3.4, current-voltage (I-V) analyses were performed with the whole-cell patch clamp technique following the method used to establish the Ca^{2+} permeability of *N*-methyl-D-aspartate-type and kainate-type iGluR channels (Mayer and Westbrook, 1987; Egebjerg and Heinemann, 1993). Figure 3A shows currents during three selected voltage steps from a holding potential of −70 mV before, during, and after the Asn treatment. Subtracting either the pretreatment or post-treatment current from the Asn-treated current at each clamp voltage produced a difference curve that represented the I-V characteristics of

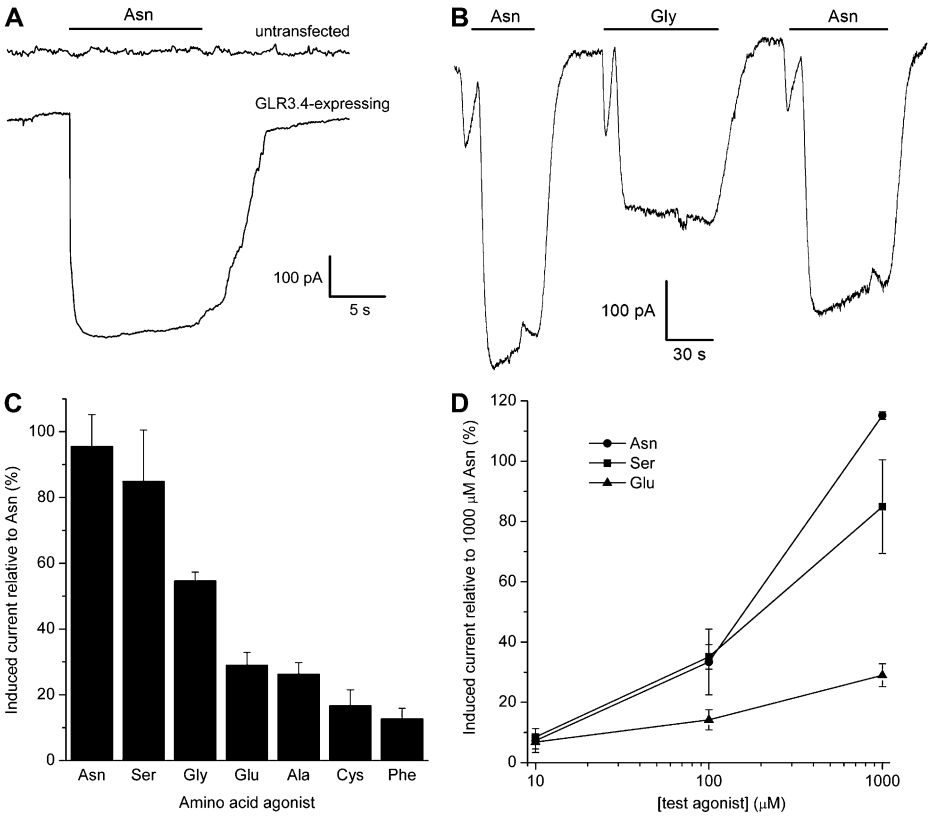

Figure 2. Agonist profile of GLR3.4 expressed in HEK cells shown by whole-cell patch clamping. A, Asn-induced inward current across the plasma membrane of a HEK cell expressing GLR3.4 is represented as a downward deflection. No such response was observed in untransfected control cells. Voltage was clamped at −70 mV. B, Sequential exposures to different amino acids in an A-B-A pattern showed a lack of GLR3.4 desensitization and permitted quantification of relative agonist effectiveness. Voltage was clamped at −70 mV. C, Magnitude of amino acid-induced current relative to a preceding response evoked by 1 mM Asn. Each determination of relative effectiveness was performed on a separate cell and each result plotted is the mean ± SEM of three or more separate experiments. D, Concentration dependence of current response induced by Asn, Ser, or Glu relative to the response subsequently invoked by 1,000 μM Asn in the same cell. The plotted data are means ± SEM, $n = 3$ different cells at each concentration.

the Asn-gated conductance (Fig. 3B). Whether pre- or post-treatment data were used as the reference state, the results were substantively the same, because there was very little desensitization of the system. With 2 mM $CaCl_2$ in the bath, inward currents larger than 100 pA were observed over much of the voltage range, even at 0 mV, where Na^+ and Cl^- would be in equilibrium based on their equal inside and outside concentrations (Fig. 3B). The difference I-V curve appeared to reverse (I = 0 pA) at 100 mV, approaching the equilibrium potential for Ca^{2+} (127 mV if $[Ca^{2+}]$ inside is 0.1 μM), indicating a high selectivity for Ca^{2+} over Na^+ or Cl^-, both of which have equilibrium potentials of 0 mV. Increasing extracellular $CaCl_2$ to 20 mM in the continuous presence of Asn doubled the inward current over most of the voltage range, as expected only if Ca^{2+} were the predominantly permeable ion. A positive shift in reversal potential expected after switching to higher external $CaCl_2$ concentration was not observed. Instead, the curve reversed at 75 mV. Still far more positive than the Na^+ or Cl^- equilibrium potentials and therefore indicative of a high Ca^{2+} permeability, the negative shift in reversal potential indicated that the GLR3.4 channel was less selective for Ca^{2+} over Na^+ in 20 mM Ca^{2+} than in 2 mM Ca^{2+}. Following the analytical methods of either Lewis (1979) or Lee and Tsien (1984), selectivity for Ca^{2+} over Na^+ was calculated to drop from 5×10^4 to 7×10^2 when external Ca^{2+} was raised from 2 mM to 20 mM. Cells transfected with a vector not containing GLR3.4 responded very little to Asn or to increasing $CaCl_2$ concentration; the difference I-V curves reversed near 0 mV (Fig. 3B). Each individual trial summarized in Figure 3B is presented in Supplemental File S1.

The above results indicate that GLR3.4 encodes a Ca^{2+}-permeable, Asn/Ser,Gly-gated ion channel. This conclusion was independently tested by monitoring cytoplasmic Ca^{2+} concentration. The fluorescent marker protein separately encoded by the transfection vector was the YC3.6 Ca^{2+} indicator protein, permitting cytoplasmic Ca^{2+} concentration to be monitored by measuring the ratio of YC3.6 fluorescence intensity at two wavelengths with a confocal microscope. Figure 3C shows that Asn triggered a large, transient rise in cytoplasmic Ca^{2+} concentration in HEK cells expressing GLR3.4 but not in cells expressing only the YC3.6 Ca^{2+} sensor. Figure 3D shows similar transient responses to Gly in three separate cells expressing GLR3.4. Cytoplasmic Ca^{2+} concentration rose and returned to baseline within approximately 1 min after amino acid treatment, as observed in the plant (Dennison and Spalding, 2000; Dubos et al., 2003; Meyerhoff et al., 2005; Qi et al., 2006). The patch clamp results show that GLR3.4 channel activity was sustained, not transient. Presumably, active Ca^{2+} transport systems reset the resting levels in the HEK cell as in the plant (Spalding and Harper, 2011). Unlike the results in Figure 2, which could be internally normalized, Figure 3 results are subject to variability in GLR3.4 expression levels between individual cells, as shown in Figure 3D.

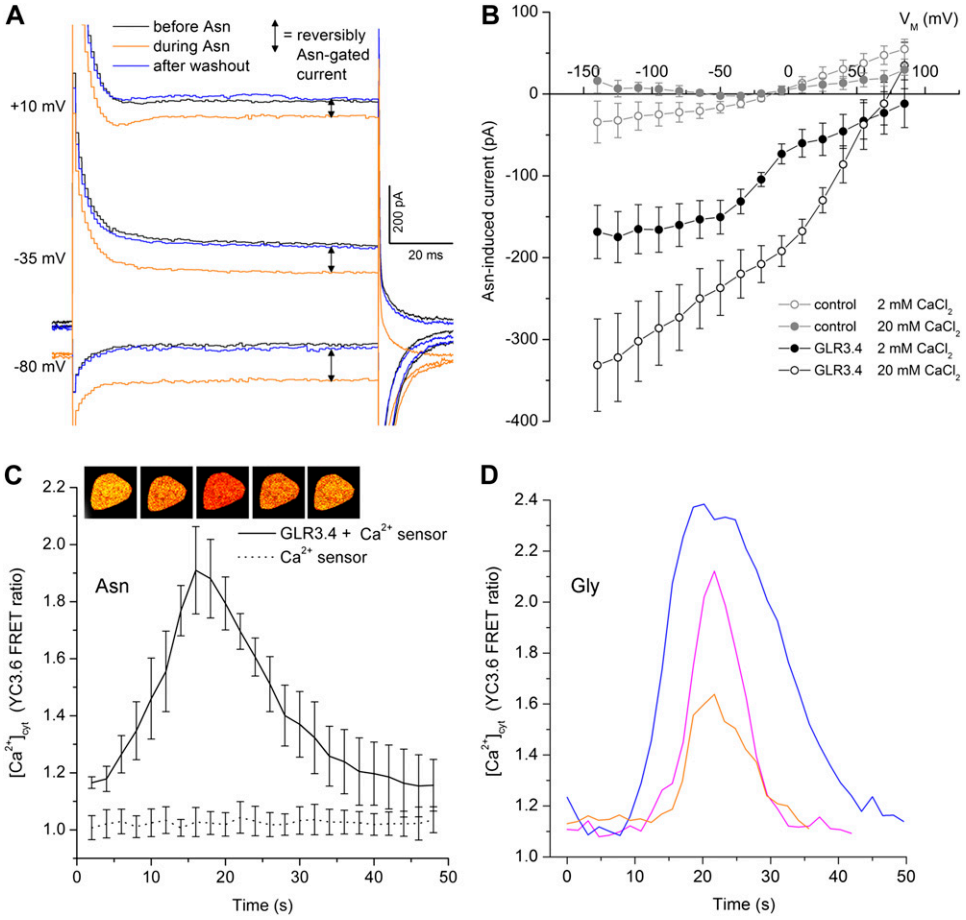

Figure 3. Ca^{2+} permeability of GLR3.4 channels expressed in HEK cells shown by whole-cell patch clamping and live-cell Ca^{2+} imaging. A, Whole-cell current traces recorded from a HEK cell expressing GLR3.4 subjected to a voltage-step protocol before (black), during 2 mM Asn treatment (orange), and after agonist washout (blue). The voltage across the membrane was clamped at values ranging from −140 to +85mV in 15-mV increments for 100 ms each, with a 0.8-s recovery period at −70 mV between steps, but only three steps were selected for display. The magnitude of the current reversibly gated by agonist (difference current) is indicated by arrows. B, Difference current-voltage relationship of GLR3.4-expressing or control cells bathed in a NaCl-based buffer containing 2 or 20 mM $CaCl_2$. Control cells were transfected with the YC3.6 Ca^{2+} indicator only. The plotted data are means ± SEM, n = 5 for control, n = 6 for *GLR3.4* transfected cells. C, Cytoplasmic Ca^{2+} rise triggered by Asn in HEK cells expressing GLR3.4 and the optical Ca^{2+} sensor YC3.6 or only YC3.6. The 535:480 nm fluorescence ratio, a direct measure of cytoplasmic Ca^{2+} concentration, rose transiently upon application of 500 μM Asn only in cells expressing GLR3.4. The values are means ± SEM, $n \geq 3$. Above the plots are confocal microscope images falsely colored to represent the magnitude of the FRET signal at each pixel at selected time points in a representative series. D, Cytoplasmic Ca^{2+} rise triggered by Gly in HEK cells expressing GLR3.4 and the optical Ca^{2+} sensor YC3.6. Three independent trials are shown.

The results in Figures 2 and 3, along with previous in planta results (Qi et al., 2006; Stephens et al., 2008), indicate that GLR3.4 is activated by amino acids to admit Ca^{2+} into the cytoplasm to create a transient rise in Ca^{2+} concentration.

DISCUSSION

In the years since *GLR* genes were discovered in plants (Lam et al., 1998; Lacombe et al., 2001), research has focused on their phylogeny and evolution (Chiu et al., 1999, 2002; Turano et al., 2001), expression patterns and transcriptional responses (Chiu et al., 2002; Meyerhoff et al., 2005; Roy et al., 2008), roles in carbon to nitrogen balance (Kang and Turano, 2003), abscisic acid sensing (Kang et al., 2004), control of root growth (Li et al., 2006; Miller et al., 2010), and contributions to ionic relations including Ca^{2+} signaling (Kim et al., 2001; Dubos et al., 2003; Meyerhoff et al., 2005; Kang et al., 2006; Qi et al., 2006; Cho et al., 2009). Slowest to accrue has been information about the intrinsic transport properties of a GLR protein (Dietrich et al., 2010). Heterologous expression followed by voltage-clamp analysis is typically the most reliable source of this information. As a result of that approach in the current study, the evidence indicating that GLRs encode Ca^{2+} channels is now independently 2-fold: mutating a *GLR*

impairs amino acid-gated Ca^{2+} influx and membrane depolarization in the plant (Qi et al., 2006; Stephens et al., 2008) and adding a GLR to a HEK cell creates an amino acid-gated Ca^{2+} conductance capable of generating a cytoplasmic Ca^{2+} signal (Figs. 2 and 3). Substantiating a Ca^{2+}-permeable channel in plants with these two independent forms of evidence is significant because Ca^{2+} signals regulate numerous physiological and developmental processes, yet components of the generative mechanisms are insufficiently understood at the molecular level (McAinsh and Pittman, 2009; Dodd et al., 2010; Spalding and Harper, 2011). Now there seems to be little room for doubt that GLR3.4 and probably other family members function as amino acid-gated, Ca^{2+}-permeable channels that are capable of generating a cytoplasmic Ca^{2+} signal.

This may be the extent of the similarity between plant GLRs and animal iGluRs. GLR3.4 is activated by at least three structurally diverse amino acids (Asn, Ser, and Gly) and thus displays an agonist profile broader than any iGluR. This may be because of the different evolutionary origins of the amino termini of GLRs and iGluRs (Turano et al., 2001), which in the case of GLRs may harbor additional amino acid binding sites (Acher and Bertrand, 2005). Also, the poor selectivity between cations characteristic of iGluRs is not shared by GLR3.4, which is shown here to be highly selective for Ca^{2+} over Na^{+} in standard HEK cell recording conditions. The unique pore sequences of GLRs probably account for this difference and may present opportunities to learn about the structural basis of Ca^{2+} selectivity in channels. Because selectivity of GLR3.4 can be influenced by external Ca^{2+} concentration (Fig. 3B), possibly through effects on surface charges near the entrance to the conduction pathway or block by divalent cations (Mayer and Westbrook, 1987), future research should examine selectivity in ionic conditions similar to those prevailing in the plant apoplast. A Ca^{2+}-dependent decrease in Ca^{2+} selectivity over Na^{+} in Glu receptors has been observed before (Jatzke et al., 2002). The phenomenon was suggested to make Ca^{2+} influx less dependent on variations in extracellular Ca^{2+} concentration (Jahr and Stevens, 1993). No physiological significance of this effect to plants can be asserted, given that GLR3.4 probably never naturally experiences more than 1% to 10% of the 20 mM external Ca^{2+} used to verify Ca^{2+} permeability in Figure 3B.

The 20 different GLR subunits encoded in the Arabidopsis genome could theoretically form 8,855 unique tetramers. Any tetramer containing a GLR3.4 subunit is predicted to be gated by Asn, Gly, or Ser as a result of the present work (Fig. 2) and the earlier finding that in planta responses to these same three amino acids are specifically impaired by *glr3.4* mutations (Stephens et al., 2008). Such predictions can be directly tested now that HEK cells have been established as a system for studying GLR function. The subunits to coexpress and test electrophysiologically could be selected on the basis of colocalization of expression in the plant (Chiu et al., 2002; Roy et al., 2008; Dietrich et al., 2010). Any new gating or transport features displayed by heteromeric channels may provide clues about their physiological functions in the plant.

Considering scenarios in which the GLR3.4 agonists Asn, Ser, and Gly could be significantly present in the apoplast and therefore effective gating agents is another means of generating hypotheses about physiological function. Asn and Ser and other amino acids are exuded by plant roots (Nguyen, 2003). GLR3.4 and other members of the GLR family are expressed in roots (Chiu et al., 2002; Roy et al., 2008; Dietrich et al., 2010). Exuded amino acids that reach the rhizosphere are believed to be quickly mineralized by microbial metabolism (Griffiths et al., 1999; Owen and Jones, 2001). Perhaps the combination of exudation and microbial metabolism creates local amino acid patterns in the rhizosphere that act as signals transduced by Ca^{2+}-permeable GLRs to influence root physiology or development. The GLR3.4 agonists Asn and Ser and other amino acids are also present in the xylem at concentrations that depend on carbon and nitrogen status. Because the xylem is in diffusional contact with the apoplast, GLRs could relate C:N metabolism status to cells via Ca^{2+} signals. Studies of *glr* mutant phenotypes that include manipulation of apoplastic agonist concentrations or patterns may uncover higher level physiological functions of amino acid-gated, Ca^{2+}-permeable channels.

MATERIALS AND METHODS

Plant Material

The Arabidopsis Genome Initiative locus identifier for *GLR3.4* is At1g05200. T-DNA insertion lines for *glr3.4-1* (Salk_079842); *glr3.4-2* (Salk_016904) were obtained from the Salk Institute (http://signal.salk.edu/cgi-bin/tdnaexpress). Seeds of Arabidopsis (*Arabidopsis thaliana*) were surface sterilized and sown on petri plates containing 0.5× Murashige and Skoog salts, 0.5% Suc (w/v), and 23 mM MES, adjusted to pH 5.7 with KOH and gelled with 1% agarose.

DNA Cloning

Full-length *GLR3.4* cDNA was isolated from total RNA by reverse transcription-PCR using the Superscript First-Strand System for reverse transcription-PCR and AccuPrime Pfx DNA Polymerase (Invitrogen) with the following amplification primers: forward, 5′-cat gtc tac *gct agc* atg gga ttt ttg gtg atg at-3′; reverse, 5′-cat gtc tac *ccc ggg* tta agt aat ttc gcc atg ttg tga ttg-3′, with *Nhe*I and *Xma*I restriction sites within primers italicized. The resulting PCR fragment was cloned into TOPO vector (*pCR2.1*) following the manufacturer's protocol (Invitrogen). Verified *pCR2.1-GLR3.4* clone was digested with *Nhe*I and *Xma*I and subcloned into the modified mammalian expression vector *pIRES2-EGFP2* (Clontech) in which the enhanced GFP (EGFP) fragment was replaced with yellow cameleon *YC3.60* (*pIRES2-YC3.6*), generating the resulting construct *pIRES2-YC3.6 GLR3.4* used for HEK cell expression.

To generate the *GFP-GLR3.4* fusion constructs, the full-length cDNA of *GLR3.4* was amplified as described above using the following amplification primers: forward, 5′ *-cacc* at ggg att ttt ggt gat gat aag aga agt ttc-3′; reverse, 5′-agt aat ttc gcc atg ttg tga ttg-3′. The gateway directional cloning modification (CACC) in italics was added at the 5′ end of the forward primer. The resulting PCR fragment was cloned into the pENTR-D entry vector (Invitrogen) followed by a GATEWAY recombination reaction (Invitrogen) into pcDNA-DEST47 mammalian expression vector (pcDEST47-GLR3.4-GFP; for transfection of HEK 293T cells) or the modified pEARLEYGATE 102 plant expression vector (Earley et al., 2006) in which the cyan fluorescent protein fragment was replaced with EGFP for enhanced fluorescence to produce the

respective *35S:GLR3.4-EGFP*. The floral dip method was used to transform the *glr3.4-1* mutant with the *35S:GLR3.4-EGFP* construct.

HEK Cell Culture and Transfection

HEK293T cells were cultured in Dulbecco's modified Eagle's medium supplemented with 10% fetal bovine serum, 100 IU/mL of penicillin, and 100 μg/mL of streptomycin. Trypsin-treated HEK293T cells were seeded onto glass coverslips 8 h to 1 d before transfection and placed in a 37°C incubator with 95% air and 5% CO_2. Transfections were performed using FuGENE 6 Transfection Reagent (Roche Scientific). Cells were patch-clamped 48 h after transfection.

Electrophysiology

Transfected HEK cells were incubated in Hank's balanced buffered solution 45 to 60 min prior to experimentation to dilute any remaining amino acid-rich culture solution. HEK cells expressing the GLR3.4 construct were identified by visualizing the YC3.6 coexpressed marker with the fluorescence microscope on which the patch clamp apparatus was based (Olympus BX51WI upright fixed stage microscope equipped with a 40× dipping lens). Cells showing a strong fluorescence signal were selected for whole-cell patch clamp analysis. Membrane currents were recorded after achieving the whole-cell configuration using an Axopatch 200A patch clamp amplifier and digitized using a Digidata 1440A A/D board controlled by pCLAMP 10.2 software (Molecular Devices, www.moleculardevices.com). The currents were low-pass filtered at 5 kHz and digitized at 10 KHz. The bathing solution contained (mM): 138 NaCl, 5.3 KCl, 1 $CaCl_2$, 10 HEPES and 5.5 D-Glc, 0.4 KH_2PO_4, and 0.3 Na_2HPO_4 adjusted to pH 7.3 with NaOH, with or without the indicated amino acid. The pipette solution contained (mM): 140 NaCl, 10 EGTA, 5 D-Glc, 1 Mg-ATP, and 10 HEPES, adjusted to pH 7.3 with NaOH. To investigate Ca^{2+} conductance, the bathing solution was modified to contain (mM): 140 NaCl, 5 D-Glc, 2 or 20 $CaCl_2$, 10 HEPES adjusted to pH 7.3 with NaOH.

Measurement of Cytosolic Ca^{2+} Using YC3.6

HEK293T cells transiently expressing the yellow cameleon YC3.6, adherent on glass coverslips, were submerged in 1 mL of the bathing solution described above. Test agonist was added as a concentrated stock to the 1 mL chamber to achieve the indicated final concentration. The YC3.6 Förster resonance energy transfer (FRET) signal (ratio of 480:535 nm fluorescence) image was acquired at 1 Hz using the Meta detector of a Zeiss LSM 510 confocal microscope. The FRET ratios at all the pixels in a region of interest within the cell were averaged to quantify the amino acid-induced Ca^{2+} rise.

Subcellular Localization

A Zeiss 510 laser scanning confocal microscope was used to visualize *GLR3.4-EGFP* in leaf epidermal cells and in HEK293T cells. Treatment with propidium iodide (50 μg mL^{-1}) for 5 min stained the plant cell walls. The samples were excited with the 488-nm laser line and channel mode detection was used to record the emission of EGFP (500–530 nm) and propidium iodide (560 nm). For plasmolysis experiments, leaf epidermal strips were submerged in 0.7 M sorbitol for 5 to 20 min before the microscopy was performed. Optics employed were a plan-Apochromat 20× lens or a C-Apochromat 40× water immersion lens. HEK293T cells grown on glass coverslips and transiently transfected with the pcDEST47-GLR3.4-GFP vector were visualized 48 h later. As a control, the pcDEST47 empty vector was used.

Supplemental Data

The following materials are available in the online version of this article.

Supplemental File S1. I-V data used to generate Figure 3B.

Received March 20, 2012; accepted March 23, 2012; published March 23, 2012.

LITERATURE CITED

Acher FC, Bertrand HO (2005) Amino acid recognition by Venus flytrap domains is encoded in an 8-residue motif. Biopolymers **80:** 357–366

Chazot PL, Cik M, Stephenson FA (1999) Transient expression of functional NMDA receptors in mammalian cells. *In* M Li, ed, NMDA Receptor Protocols: Methods in Molecular Biology, Vol 128. Humana Press, Totowa, NJ, pp 33–42

Chiu J, DeSalle R, Lam HM, Meisel L, Coruzzi G (1999) Molecular evolution of glutamate receptors: a primitive signaling mechanism that existed before plants and animals diverged. Mol Biol Evol **16:** 826–838

Chiu JC, Brenner ED, DeSalle R, Nitabach MN, Holmes TC, Coruzzi GM (2002) Phylogenetic and expression analysis of the glutamate-receptor-like gene family in Arabidopsis thaliana. Mol Biol Evol **19:** 1066–1082

Cho D, Kim SA, Murata Y, Lee S, Jae SK, Nam HG, Kwak JM (2009) Deregulated expression of the plant glutamate receptor homolog AtGLR3.1 impairs long-term Ca^{2+}-programmed stomatal closure. Plant J **58:** 437–449

Christopher DA, Borsics T, Yuen CY, Ullmer W, Andème-Ondzighi C, Andres MA, Kang BH, Staehelin LA (2007) The cyclic nucleotide gated cation channel AtCNGC10 traffics from the ER via Golgi vesicles to the plasma membrane of Arabidopsis root and leaf cells. BMC Plant Biol **7:** 48

Davenport R (2002) Glutamate receptors in plants. Ann Bot (Lond) **90:** 549–557

Demidchik V, Davenport RJ, Tester M (2002) Nonselective cation channels in plants. Annu Rev Plant Biol **53:** 67–107

Demidchik V, Essah PA, Tester M (2004) Glutamate activates cation currents in the plasma membrane of Arabidopsis root cells. Planta **219:** 167–175

Dennison KL, Spalding EP (2000) Glutamate-gated calcium fluxes in Arabidopsis. Plant Physiol **124:** 1511–1514

Dietrich P, Anschütz U, Kugler A, Becker D (2010) Physiology and biophysics of plant ligand-gated ion channels. Plant Biol (Stuttg) (Suppl 1) **12:** 80–93

Dodd AN, Kudla J, Sanders D (2010) The language of calcium signaling. Annu Rev Plant Biol **61:** 593–620

Dravid SM, Prakash A, Traynelis SF (2008) Activation of recombinant NR1/NR2C NMDA receptors. J Physiol **586:** 4425–4439

Dubos C, Huggins D, Grant GH, Knight MR, Campbell MM (2003) A role for glycine in the gating of plant NMDA-like receptors. Plant J **35:** 800–810

Earley KW, Haag JR, Pontes O, Opper K, Juehne T, Song K, Pikaard CS (2006) Gateway-compatible vectors for plant functional genomics and proteomics. Plant J **45:** 616–629

Egebjerg J, Heinemann SF (1993) Ca^{2+} permeability of unedited and edited versions of the kainate selective glutamate receptor GluR6. Proc Natl Acad Sci USA **90:** 755–759

Griffiths BS, Ritz K, Ebblewhite N, Dobson G (1999) Soil microbial community structure: effects of substrate loading rates. Soil Biol Biochem **31:** 145–153

Hollmann M, O'Shea-Greenfield A, Rogers SW, Heinemann S (1989) Cloning by functional expression of a member of the glutamate receptor family. Nature **342:** 643–648

Jahr CE, Stevens CF (1993) Calcium permeability of the *N*-methyl-D-aspartate receptor channel in hippocampal neurons in culture. Proc Natl Acad Sci USA **90:** 11573–11577

Jatzke C, Watanabe J, Wollmuth LP (2002) Voltage and concentration dependence of $Ca^{(2+)}$ permeability in recombinant glutamate receptor subtypes. J Physiol **538:** 25–39

Kang J, Turano FJ (2003) The putative glutamate receptor 1.1 (AtGLR1.1) functions as a regulator of carbon and nitrogen metabolism in *Arabidopsis thaliana*. Proc Natl Acad Sci USA **100:** 6872–6877

Kang JM, Mehta S, Turano FJ (2004) The putative glutamate receptor 1.1 (AtGLR1.1) in *Arabidopsis thaliana* regulates abscisic acid biosynthesis and signaling to control development and water loss. Plant Cell Physiol **45:** 1380–1389

Kang S, Kim HB, Lee H, Choi JY, Heu S, Oh CJ, Kwon SI, An CS (2006) Overexpression in Arabidopsis of a plasma membrane-targeting glutamate receptor from small radish increases glutamate-mediated Ca^{2+} influx and delays fungal infection. Mol Cells **21:** 418–427

Keinänen K, Wisden W, Sommer B, Werner P, Herb A, Verdoorn TA, Sakmann B, Seeburg PH (1990) A family of AMPA-selective glutamate receptors. Science **249:** 556–560

Kim SA, Kwak JM, Jae SK, Wang MH, Nam HG (2001) Overexpression of the *AtGluR2* gene encoding an Arabidopsis homolog of mammalian glutamate receptors impairs calcium utilization and sensitivity to ionic stress in transgenic plants. Plant Cell Physiol **42:** 74–84

Lacombe B, Becker D, Hedrich R, DeSalle R, Hollmann M, Kwak JM, Schroeder JI, Le Novère N, Nam HG, Spalding EP, et al (2001) The identity of plant glutamate receptors. Science **292:** 1486–1487

Lam HM, Chiu J, Hsieh MH, Meisel L, Oliveira IC, Shin M, Coruzzi G (1998) Glutamate-receptor genes in plants. Nature **396:** 125–126

Lee KS, Tsien RW (1984) High selectivity of calcium channels in single dialysed heart cells of the guinea-pig. J Physiol **354:** 253–272

Lewis CA (1979) Ion-concentration dependence of the reversal potential and the single channel conductance of ion channels at the frog neuromuscular junction. J Physiol **286:** 417–445

Li J, Zhu S, Song X, Shen Y, Chen H, Yu J, Yi K, Liu Y, Karplus VJ, Wu P, Deng XW (2006) A rice glutamate receptor-like gene is critical for the division and survival of individual cells in the root apical meristem. Plant Cell **18:** 340–349

Mayer ML, Westbrook GL (1987) Permeation and block of N-methyl-D-aspartic acid receptor channels by divalent cations in mouse cultured central neurones. J Physiol **394:** 501–527

McAinsh MR, Pittman JK (2009) Shaping the calcium signature. New Phytol **181:** 275–294

Meyerhoff O, Müller K, Roelfsema MR, Latz A, Lacombe B, Hedrich R, Dietrich P, Becker D (2005) AtGLR3.4, a glutamate receptor channel-like gene is sensitive to touch and cold. Planta **222:** 418–427

Michard E, Lima PT, Borges F, Silva AC, Portes MT, Carvalho JE, Gilliham M, Liu LH, Obermeyer G, Feijó JA (2011) Glutamate receptor-like genes form Ca^{2+} channels in pollen tubes and are regulated by pistil D-serine. Science **332:** 434–437

Mikosch M, Käberich K, Homann U (2009) ER export of KAT1 is correlated to the number of acidic residues within a triacidic motif. Traffic **10:** 1481–1487

Miller ND, Durham Brooks TL, Assadi AH, Spalding EP (2010) Detection of a gravitropism phenotype in *glutamate receptor-like 3.3* mutants of *Arabidopsis thaliana* using machine vision and computation. Genetics **186:** 585–593

Monyer H, Sprengel R, Schoepfer R, Herb A, Higuchi M, Lomeli H, Burnashev N, Sakmann B, Seeburg PH (1992) Heteromeric NMDA receptors: molecular and functional distinction of subtypes. Science **256:** 1217–1221

Nguyen C (2003) Rhizodeposition of organic C by plants: mechanisms and controls. Agronomie **23:** 375–396

Owen AG, Jones DL (2001) Competition for amino acids between wheat roots and rhizosphere microorganisms and the role of amino acids in plant N acquisition. Soil Biol Biochem **33:** 651–657

Qi Z, Stephens NR, Spalding EP (2006) Calcium entry mediated by GLR3.3, an Arabidopsis glutamate receptor with a broad agonist profile. Plant Physiol **142:** 963–971

Roy SJ, Gilliham M, Berger B, Essah PA, Cheffings C, Miller AJ, Davenport RJ, Liu L-H, Skynner MJ, Davies JM, et al (2008) Investigating glutamate receptor-like gene co-expression in *Arabidopsis thaliana*. Plant Cell Environ **31:** 861–871

Spalding EP, Harper JF (2011) The ins and outs of cellular Ca^{2+} transport. Curr Op Plant Biol doi:10.1016/j.pbi.2011.08.001

Stephens NR, Qi Z, Spalding EP (2008) Glutamate receptor subtypes evidenced by differences in desensitization and dependence on the *GLR3.3* and *GLR3.4* genes. Plant Physiol **146:** 529–538

Tang RH, Han S, Zheng H, Cook CW, Choi CS, Woerner TE, Jackson RB, Pei ZM (2007) Coupling diurnal cytosolic Ca^{2+} oscillations to the CAS-IP3 pathway in Arabidopsis. Science **315:** 1423–1426

Tapken D, Hollmann M (2008) *Arabidopsis thaliana* glutamate receptor ion channel function demonstrated by ion pore transplantation. J Mol Biol **383:** 36–48

Teardo E, Formentin E, Segalla A, Giacometti GM, Marin O, Zanetti M, Lo Schiavo F, Zoratti M, Szabò I (2011) Dual localization of plant glutamate receptor AtGLR3.4 to plastids and plasmamembrane. Biochim Biophys Acta **1807:** 359–367

Traynelis SF, Wollmuth LP, McBain CJ, Menniti FS, Vance KM, Ogden KK, Hansen KB, Yuan H, Myers SJ, Dingledine R (2010) Glutamate receptor ion channels: structure, regulation, and function. Pharmacol Rev **62:** 405–496

Turano FJ, Panta GR, Allard MW, van Berkum P (2001) The putative glutamate receptors from plants are related to two superfamilies of animal neurotransmitter receptors via distinct evolutionary mechanisms. Mol Biol Evol **18:** 1417–1420

Zhang S, Huganir RL (1999) Calmodulin modification of NMDA receptors. *In* M Li, ed. NMDA Receptor Protocols: Methods in Molecular Biology, Vol 128. Humana Press, Totowa, NJ, pp 103–111.